Biomedical Optics EXPRESS

Spectrally encoded confocal microscopy of esophageal tissues at 100 kHz line rate

Simon C. Schlachter,[1,4] DongKyun Kang,[1,4] Michalina J. Gora,[1] Paulino Vacas-Jacques,[1] Tao Wu,[1] Robert W. Carruth,[1] Eric J. Wilsterman,[1] Brett E. Bouma,[1,2] Kevin Woods,[1] and Guillermo J. Tearney[1,2,3,*]

[1]*Harvard Medical School and Wellman Center for Photomedicine, Massachusetts General Hospital, 55 Fruit Street, Boston, MA 02114, USA*

[2]*Harvard-MIT Division of Health Sciences and Technology, 77 Massachusetts Avenue, Cambridge, MA 02139, USA*

[3]*Department of Pathology, Harvard Medical School and Massachusetts General Hospital, 55 Fruit Street, Boston, MA 02114, USA*

[4]*These authors contributed equally to this work.*

[*]*gtearney@partners.org*

Abstract: Spectrally encoded confocal microscopy (SECM) is a reflectance confocal microscopy technology that uses a diffraction grating to illuminate different locations on the sample with distinct wavelengths. SECM can obtain line images without any beam scanning devices, which opens up the possibility of high-speed imaging with relatively simple probe optics. This feature makes SECM a promising technology for rapid endoscopic imaging of internal organs, such as the esophagus, at microscopic resolution. SECM imaging of the esophagus has been previously demonstrated at relatively low line rates (5 kHz). In this paper, we demonstrate SECM imaging of large regions of esophageal tissues at a high line imaging rate of 100 kHz. The SECM system comprises a wavelength-swept source with a fast sweep rate (100 kHz), high output power (80 mW), and a detector unit with a large bandwidth (100 MHz). The sensitivity of the 100-kHz SECM system was measured to be 60 dB and the transverse resolution was 1.6 μm. Excised swine and human esophageal tissues were imaged with the 100-kHz SECM system at a rate of 6.6 mm^2/sec. Architectural and cellular features of esophageal tissues could be clearly visualized in the SECM images, including papillae, glands, and nuclei. These results demonstrate that large-area SECM imaging of esophageal tissues can be successfully conducted at a high line imaging rate of 100 kHz, which will enable whole-organ SECM imaging *in vivo*.

OCIS codes: (170.1790) Confocal microscopy; (170.2680) Gastrointestinal; (170.4730) Optical pathology.

References and links

1. A. L. Polglase, W. J. McLaren, S. A. Skinner, R. Kiesslich, M. F. Neurath, and P. M. Delaney, "A fluorescence confocal endomicroscope for in vivo microscopy of the upper- and the lower-GI tract," Gastrointest. Endosc. **62**(5), 686–695 (2005).
2. R. Kiesslich, L. Gossner, M. Goetz, A. Dahlmann, M. Vieth, M. Stolte, A. Hoffman, M. Jung, B. Nafe, P. R. Galle, and M. F. Neurath, "In vivo histology of Barrett's esophagus and associated neoplasia by confocal laser endomicroscopy," Clin. Gastroenterol. Hepatol. **4**(8), 979–987 (2006).
3. S. Kitabatake, Y. Niwa, R. Miyahara, A. Ohashi, T. Matsuura, Y. Iguchi, Y. Shimoyama, T. Nagasaka, O. Maeda, T. Ando, N. Ohmiya, A. Itoh, Y. Hirooka, and H. Goto, "Confocal endomicroscopy for the diagnosis of gastric cancer in vivo," Endoscopy **38**(11), 1110–1114 (2006).
4. A. M. Buchner, M. W. Shahid, M. G. Heckman, M. Krishna, M. Ghabril, M. Hasan, J. E. Crook, V. Gomez, M. Raimondo, T. Woodward, H. C. Wolfsen, and M. B. Wallace, "Comparison of probe-based confocal laser endomicroscopy with virtual chromoendoscopy for classification of colon polyps," Gastroenterology **138**(3), 834–842 (2010).
5. V. Becker, T. Vercauteren, C. H. von Weyhern, C. Prinz, R. M. Schmid, and A. Meining, "High-resolution miniprobe-based confocal microscopy in combination with video mosaicing (with video)," Gastrointest. Endosc. **66**(5), 1001–1007 (2007).

#192677 - $15.00 USD Received 21 Jun 2013; revised 1 Aug 2013; accepted 5 Aug 2013; published 13 Aug 2013

6. G. J. Tearney, R. H. Webb, and B. E. Bouma, "Spectrally encoded confocal microscopy," Opt. Lett. **23**(15), 1152–1154 (1998).
7. D. Yelin, C. Boudoux, B. E. Bouma, and G. J. Tearney, "Large area confocal microscopy," Opt. Lett. **32**(9), 1102–1104 (2007).
8. D. Kang, H. Yoo, P. Jillella, B. E. Bouma, and G. J. Tearney, "Comprehensive volumetric confocal microscopy with adaptive focusing," Biomed. Opt. Express **2**(6), 1412–1422 (2011).
9. D. Kang, M. J. Suter, C. Boudoux, H. Yoo, P. S. Yachimski, W. P. Puricelli, N. S. Nishioka, M. Mino-Kenudson, G. Y. Lauwers, B. E. Bouma, and G. J. Tearney, "Comprehensive imaging of gastroesophageal biopsy samples by spectrally encoded confocal microscopy," Gastrointest. Endosc. **71**(1), 35–43 (2010).
10. D. K. Kang, M. J. Suter, C. Boudoux, P. S. Yachimski, W. P. Puricelli, N. S. Nishioka, M. Mino-Kenudson, G. Y. Lauwers, B. E. Bouma, and G. J. Tearney, "Co-registered spectrally encoded confocal microscopy and optical frequency domain imaging system," J. Microsc. **239**(2), 87–91 (2010).
11. H. Yoo, D. Kang, A. J. Katz, G. Y. Lauwers, N. S. Nishioka, Y. Yagi, P. Tanpowpong, J. Namati, B. E. Bouma, and G. J. Tearney, "Reflectance confocal microscopy for the diagnosis of eosinophilic esophagitis: a pilot study conducted on biopsy specimens," Gastrointest. Endosc. **74**(5), 992–1000 (2011).
12. C. Boudoux, S. Yun, W. Oh, W. White, N. Iftimia, M. Shishkov, B. Bouma, and G. Tearney, "Rapid wavelength-swept spectrally encoded confocal microscopy," Opt. Express **13**(20), 8214–8221 (2005).
13. Y. K. Tao and J. A. Izatt, "Spectrally encoded confocal scanning laser ophthalmoscopy," Opt. Lett. **35**(4), 574–576 (2010).
14. L. Golan, D. Yeheskely-Hayon, L. Minai, and D. Yelin, "High-speed interferometric spectrally encoded flow cytometry," Opt. Lett. **37**(24), 5154–5156 (2012).
15. T. T. W. Wong, A. K. S. Lau, K. K. Y. Wong, and K. K. Tsia, "Optical time-stretch confocal microscopy at 1 μm," Opt. Lett. **37**(16), 3330–3332 (2012).
16. C. Glazowski and M. Rajadhyaksha, "Optimal detection pinhole for lowering speckle noise while maintaining adequate optical sectioning in confocal reflectance microscopes," J. Biomed. Opt. **17**(8), 085001 (2012).
17. W. Y. Oh, B. J. Vakoc, M. Shishkov, G. J. Tearney, and B. E. Bouma, ">400 kHz repetition rate wavelength-swept laser and application to high-speed optical frequency domain imaging," Opt. Lett. **35**(17), 2919–2921 (2010).
18. W. Wieser, B. R. Biedermann, T. Klein, C. M. Eigenwillig, and R. Huber, "Multi-Megahertz OCT: High quality 3D imaging at 20 million A-scans and 4.5 GVoxels per second," Opt. Express **18**(14), 14685–14704 (2010).

1. Introduction

Confocal laser endomicroscopy (CLE) is a promising imaging technology that can provide microscopic images of the gastrointestinal (GI) organs *in vivo* [1]. CLE has been shown to visualize histomorphologic features associated with various GI diseases, including Barrett's esophagus [2], gastric cancer [3], and colorectal neoplasia [4]. The field of view (FOV) of CLE, however, is limited to approximately 0.5 by 0.5 mm^2. The small FOV makes it challenging to conduct confocal imaging of the entire tissue region that may be at risk. Recent studies showed that the FOV can be increased by manually moving the CLE probe relative to the tissue and mosaicking the images together [5]. Yet, even with these advances, CLE is only capable of imaging large luminal organs in limited focal areas. In principle, however, the FOV can be increased further, even to the size of the entire organ, if the imaging speed (i.e. line rate) can be increased significantly and if the CLE probe can be rapidly scanned in a controlled manner.

Spectrally-encoded confocal microscopy (SECM) is a reflectance confocal microscopy technology that has a potential to significantly increase the imaging speed of CLE [6]. In the SECM endoscopic probe, illumination light is diffracted by a transmission grating. Each wavelength in the illumination spectrum is diffracted at a unique angle and then focused on a distinctive transverse location on the tissue by a high-numerical aperture (NA) objective lens. When a wavelength-swept source is used, the beam scans the sample along one dimension as the wavelength is changed – scanning that occurs without any mechanical motion in the probe. This passive scanning feature of SECM makes it possible to image at a much higher rate than is possible with miniature beam scanning devices. The SECM probe can image large areas of the tissue by helically scanning the probe optics using a motor and a pull-back stage [7, 8].

The potential to achieve a high imaging rate by employing simple probe optics makes SECM attractive for high-speed endoscopic imaging of luminal organs such as the esophagus. Previously, we showed that SECM can visualize key cellular features associated with various esophageal diseases [9–11]. The translation of SECM into a clinically-useable endoscopic device for esophageal imaging, however, has been delayed in part by the imaging rate of our

#192677 - $15.00 USD Received 21 Jun 2013; revised 1 Aug 2013; accepted 5 Aug 2013; published 13 Aug 2013

previous SECM system, 5 kHz [12]. With this line imaging rate, the imaging time for SECM imaging of the entire distal esophagus (length = 50 mm; diameter around the probe = 7 mm) with a pixel size of 1 μm is about 12 minutes. This imaging time would increase the procedural time significantly, which can make it difficult to use SECM in the clinical setting. The imaging time is increased further if multiple focal planes are imaged. For example, for our case of 5 focal planes, the imaging time would he extended to one hour.

Recently, there have been several reports that describe advancement of the imaging rate of SECM. Tao *et al*. developed a spectral-domain SECM system for ophthalmologic applications using a super-luminescent diode (central wavelength = 840 nm; bandwidth = 49 nm) and a high-speed spectrometer (maximum line imaging rate = 52 kHz) [13]. This spectral-domain SECM system was successfully used for imaging the human fundus *in vivo*. Golan *et al.* developed a high-speed SECM system using a wavelength-swept source (sweeping rate = 100 kHz; power = 15 mW) and interferometric detection optics [14]. This SECM system by Golan *et al.* was successfully used to image blood cells flowing within capillaries that were located approximately 80 μm below the tissue surface. Wong *et al.* reported an even higher imaging speed, a line imaging rate of 10 MHz, using a new approach termed serial time-encoded amplified microscopy (STEAM) [15]. In this approach, the spectrum of the light reflected from the sample is encoded in time using group velocity dispersion of the detection fiber and detected by a high-speed photodetector (bandwidth = 10 GHz). The STEAM system was shown to clearly visualize cellular structures of nasopharyngeal epithelial cells.

Although these papers report high-speed SECM imaging of various tissues, high-speed, large FOV SECM imaging of internal organ tissues has not yet been shown and it has not been determined whether or not such high-speed confocal microscopy enables the visualization of key cellular microstructural features. In this paper, we report the first demonstration of SECM imaging of large esophageal tissues with a line imaging rate of 100 kHz. In order to achieve this high imaging speed, we developed a SECM system by building a 100-kHz wavelength-swept source that has a high output power and a detector unit with a large bandwidth. This system was tested using resolution standards and by imaging swine and human esophageal tissues *ex vivo*.

2. Methods

2.1 SECM system and bench top optics

Figure 1 shows the schematic of the 100-kHz SECM system. SECM bench top optics [8], previously used with our SECM system for imaging human esophageal tissues, was used to test the performance of the 100-kHz SECM system. Light from the wavelength-swept source was coupled to the bench top optics through a single-mode fiber (SMF28, Corning). In the bench top optics, the light was first collimated by a collimation lens (f = 11 mm) and then diffracted by a transmission grating (groove density = 1100 lines/mm). The diffracted light was relayed by telescope optics (two achromats; magnification = 2.4) to a water-immersion objective lens (effective NA = 0.7w; f = 5.3 mm) and focused on the specimen. Reflected light from the specimen was coupled to a multi-mode detection fiber (core diameter = 62.5 um) by a collimation lens (f = 25 mm). The multi-mode fiber was used to reduce the speckle noise [16]. The detected light was delivered to a detector unit, comprised of an avalanche photo diode (AP) and a post amplifier (A), and digitized by a data acquisition unit (DAQ; PX14400D, Signatec). The digitized data were stored to a RAID array (D). The specimen was scanned by two linear translation stages in order to obtain large-area images of the specimen.

#192677 - $15.00 USD Received 21 Jun 2013; revised 1 Aug 2013; accepted 5 Aug 2013; published 13 Aug 2013

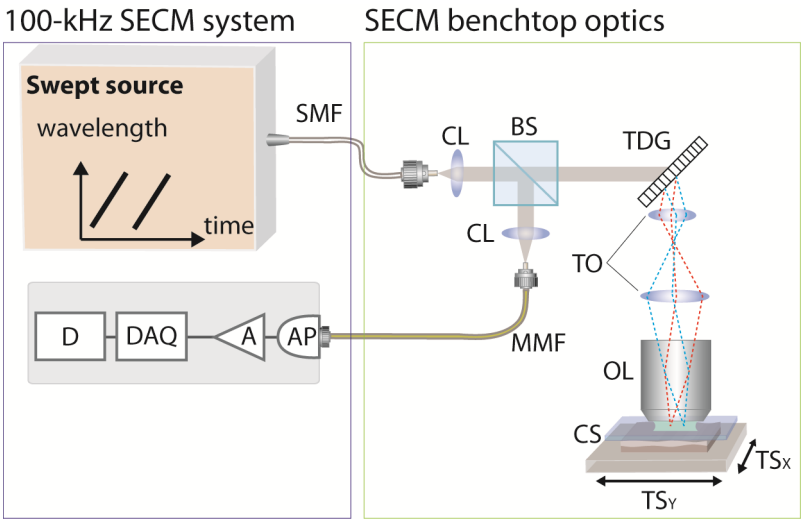

Fig. 1. Schematic of the 100-kHz SECM system. SMF – single-mode fiber; CL – collimation lens; BS – beam splitter; TDG – transmission diffraction grating; TO – telescope optics; OL – objective lens; CS – cover slip; TS – translation stage; MMF – multi-mode fiber; AP – avalanche photodiode; A – post amplifier; DAQ – data acquisition unit; D – data storage unit.

2.2 100-kHz wavelength-swept source

We have fabricated a 100-kHz wavelength-swept source based on an approach that is similar to previously developed swept sources used in high-speed optical coherence tomography [17]. In short, the wavelength sweep of the source had a duty cycle of 25%; four copies of the spectrum were multiplexed to achieve 100% duty cycle, using a previously published "cut-and-paste" scheme [17]. A detailed description of the laser is provided below.

The initial swept source spectrum was generated using a tunable filter and a fiber-based laser ring cavity. The tunable filter was comprised of a diffraction grating (DG; groove density = 830 lines/mm), telescope optics (L_1 and L_2; magnification = 1.6), two stationary mirrors, and a spinning polygon mirror (PM; number of facets = 36; rotation speed = 42,000 rpm). The tunable filter had a bandwidth of 0.12 nm and free spectral range of 440 nm. The fiber-based laser ring cavity was composed of a semiconductor optical amplifier (SOA; BOA1130S, Thorlabs) and a 50:50 free-space beam splitter (BS). The filter was adjusted to produce a duty cycle of 25%. At any given time, the laser ring cavity in conjunction with the tunable filter produced light with a very narrow bandwidth. The wavelength of the light was swept as the polygon mirror rotated. The output light from the ring cavity temporally produced a wavelength-swept spectrum with a sweep rate of 25 kHz and a duty cycle of 25%.

The 25% duty cycle wavelength swept spectrum was then pasted 3 times to create a 100% duty cycle swept source at a rate that is 4x the natural polygon filter rate (~100 kHz). First, the initial swept spectrum from the ring cavity was coupled to a polarization controller (PC) and then to a fiber isolator (FI). The tunable light was then divided into four light copies by three 50:50 fiber couplers ($FC_{50/50}$) and delivered to four fiber-optic delay lines (FDLs). Each delay line was composed of a single-mode fiber (SMF-28e + , Corning) terminated with a faraday mirror (FM). Different fiber-optic delay lines had different fiber lengths: 0, 1, 2, and 3 km. The fiber lengths were chosen so that the time delay between copies coming back from the neighboring delay lines was equal to 10 μsec, which was one quarter of the single facet-to-facet rotation time of the polygon mirror. The original and 3 copies returning from the delay lines were combined by the three fiber couplers. The combined light resulted in a wavelength-swept source with a tuning rate of 100 kHz and a duty cycle of 100%. The intensity of the light beam was amplified by a booster optical amplifier (BOA). A small portion of the output

#192677 - $15.00 USD Received 21 Jun 2013; revised 1 Aug 2013; accepted 5 Aug 2013; published 13 Aug 2013

light from the BOA was coupled to a circulator and then a fiber Bragg grating (FBG) to generate a trigger pulse for each wavelength swept spectrum.

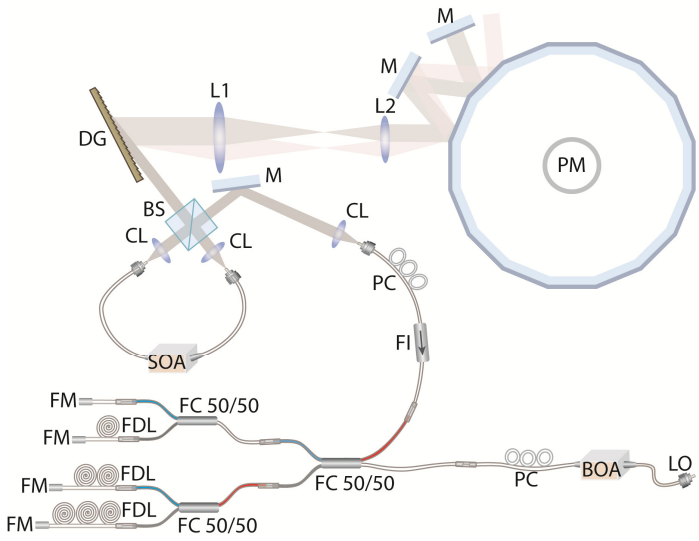

Fig. 2. Schematic of the 100-kHz wavelength-swept source. SOA – semiconductor optical amplifier; CL – collimation lens; BS – beam splitter; DG – diffraction grating; L1 and L2 – Lenses in telescope optics; M – mirror; PM – polygon mirror; PC – polarization controller; FI – fiber isolator; $FC_{50/50}$ – 50:50 fiber coupler; FDL – fiber delay line; FM – Faraday mirror; BOA – booster optical amplifier; LO – light output.

2.3 SECM detector unit

The SECM system incorporates a detector unit that uses an InGaAs avalanche photo diode (APD; PLA641, Princeton Lightwave) and a post amplifier. The APD provided an overall responsivity of 280 kV/W with a built-in transimpedance amplifier. The post amplifier was custom-designed to have a voltage gain of 6. Thus, the final responsivity of the detector unit was 1.7 MV/W. This responsivity enabled us to use the full input voltage range of the DAQ unit when imaging tissues. From our previous study of imaging human esophageal tissues with the SECM bench top system using swept source centered at 1310 nm [8], we found that the tissue reflectivity ranges between −50 and −40 dB. If we assume that the double-pass throughput of the SECM optics is around 10%, we can expect that the light power coupled to the detector unit will be between 70 and 700 nW when imaging human esophageal tissues. With a responsivity of 1.7 MW/W, the output voltage from the detector unit is between 0.12 and 1.2V. This voltage range falls within the input voltage range of the DAQ unit, ± 1.2V.

The detector unit had a large electrical bandwidth to allow high-speed SECM imaging. The APD with the built-in amplifier had a bandwidth of 150 MHz. The post amplifier was designed to have a bandwidth of 100 MHz. The SECM bench top optics had 128 resolvable points for the given grating groove density (1100 lines/mm), source spectrum (1251 – 1342 nm) and beam diameter at the grating (2.0 mm) [6]. In order to achieve Nyquist sampling, we need to sample 256 pixels per spectrally-encoded line. The sampling rate for each pixel should therefore be faster than 25.6 MHz (= 100 kHz × 256 pixels). The bandwidth of the detector unit, 100 MHz, was larger than the required sampling rate.

2.4 Data acquisition system and software

The signal from the detector unit was delivered to a high-speed DAQ unit, digitized with a bit depth of 16 bit/pixel and with a sampling rate of 120 MSamples/sec. Each SECM line was sampled using 1024 pixels. The resulting duty cycle for the data acquisition was 83%. The digitized signal was recorded by a RAID 0 hard drive array (capacity = 10 TB; max data rate

#192677 - $15.00 USD Received 21 Jun 2013; revised 1 Aug 2013; accepted 5 Aug 2013; published 13 Aug 2013

= 1400 MBytes/sec). We developed software that displays the images in real time. In the software, we generated each image frame by acquiring 1024 SECM lines. Thus, the frame rate for the image acquisition was 100 Hz. However, the frame rate for the image display was set as 30 Hz, since a frame rate higher than 30 Hz only increased the calculation burden on the system without making any perceivable difference. In order to facilitate the navigation of the large data set, the software had a mosaic view of previously-acquired images, which could be zoomed and panned. We also developed Matlab-based software that generates large-area images by stitching multiple small images. In this software, cross correlation between neighboring images was calculated. The peak position of the cross correlation curve was used to determine the offset between the neighboring images during the stitching process.

2.5 Imaging performance test

We have used standard methods to test the resolution and sensitivity of the SECM system in conjunction with the SECM bench top optics. The lateral resolution was measured by imaging the USAF resolution target and by calculating the FWHM of the Gaussian fit of the line-spread function (LSF) along the spectrally-encoded (SE) direction and its perpendicular (p-SE) direction. For each direction, the FWHM value was measured at 100 points, and the average and standard deviation of the FWHM measurement were calculated. The axial resolution was determined by measuring the FWHM of the axial response curve, the intensity response curve obtained while translating a mirror axially through the focal plane. The field curvature was measured by analyzing the axial response curve. Axial response curve was made for each transverse location. The axial coordinate of the focal point was measured for each transverse location. The field curvature was measured as the focal depth difference between the center and edge of the FOV. The sensitivity was estimated by imaging a gold mirror with a reduced illumination power (reduced by 40 dB compared to the maximum illumination power) and measuring the signal-to-noise ratio (SNR).

We imaged excised swine and human esophageal tissues to test the imaging performance. Prior to the SECM imaging, the swine tissues were treated with 6% acetic acid to enhance the nuclear contrast. This concentration of acetic acid was higher than the concentration previously used for imaging human esophageal tissues, 0.6%. The higher concentration was needed in swine tissues to obtain similar nuclear contrast enhancement to human tissue, possibly due to the difference in tissue permeability between the swine and human tissues. Human esophageal tissue obtained by endoscopic mucosal resection (EMR) was also imaged. The EMR tissue was imaged in accordance with an IRB-approved protocol (Protocol #2010-P000526.) The EMR tissue was treated with 0.6% acetic acid. After the acetic acid treatment, the tissue was placed in an imaging chamber (CoverWell, Grace Bio-labs). The thickness of the imaging chamber varied depending on the thickness of the tissue. A cover glass was placed on the tissue and imaging chamber to flatten the tissue surface. The fast translation stage moved the tissue at the speed of 70 mm/sec along the p-SE direction, resulting in the pixel size of 0.7 μm. The other translation stage moved the specimen along the SE direction at the step size of 150 μm. The imaging time for the representative imaging area of 10 mm × 10 mm was 15 sec. After the SECM imaging, the acquired images were processed to generate large-area images. The processing time for the representative image with an area of 12 mm × 12 mm was 2 minutes. SNR of the SECM image was calculated by dividing the mean intensity of the tissue portion of the image by the standard deviation of the background intensity.

#192677 - $15.00 USD Received 21 Jun 2013; revised 1 Aug 2013; accepted 5 Aug 2013; published 13 Aug 2013

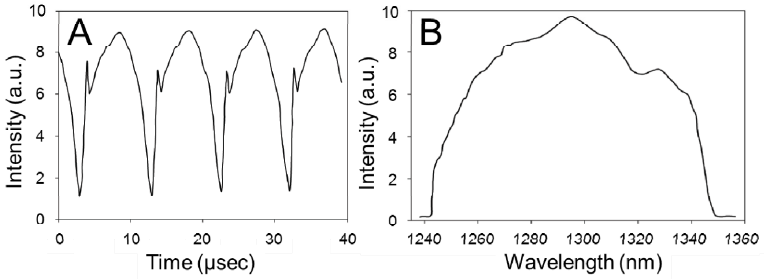

Fig. 3. Temporal variation (A) and spectrum (B) of source output.

3. Results

3.1 SECM source performance

We have tested the following characteristics of the 100-kHz swept source: average output power, sweeping rate, and spectrum. The average output power was measured to be 80 mW. The temporal variation of the output power was measured (Fig. 3(a)); results showed that the wavelength-tuning rate was 100 kHz. We measured the FWHM duty cycle by measuring the time span where the power was higher than half of the maximum power. The measured FWHM duty cycle was 83%. The spectrum of the output light was measured by using an optical spectrum analyzer (Fig. 3(b)). The FWHM of the spectrum was measured to be 91 nm centered at 1296.5 nm.

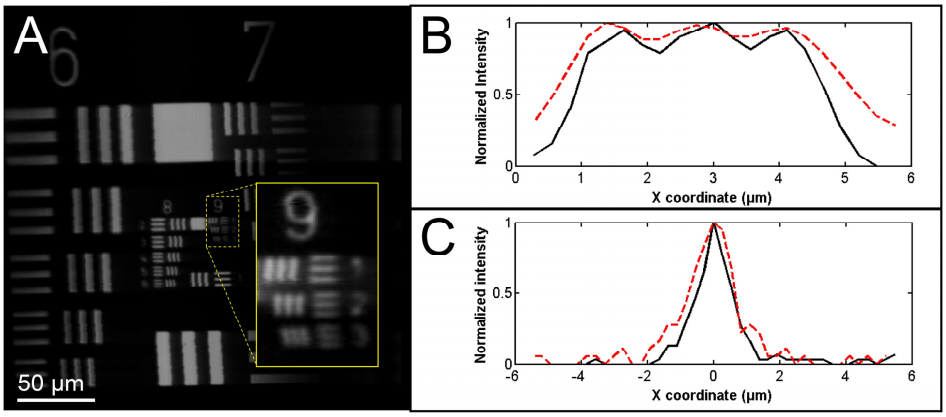

Fig. 4. Lateral resolution measurement. A - SECM image of the USAF resolution target; B – line profiles crossing the three lines at the group 9, element 3; and C – representative LSF curves. In Fig. A, horizontal direction is the spectrally-encoded direction. In Figs B and C, red dotted curves are for SE direction, and black curves are for p-SE direction.

3.2 Resolution and sensitivity

The SECM image of a USAF resolution target is shown in Fig. 4(a). The lines at the group 9, element 3 (linewidth = 0.78 μm) were resolved. Line profiles crossing the lines at the group 9, element 3 are shown in Fig. 4(b). Three peaks are clearly visible in both SE (red dotted curve) and p-SE (black curve) curves. The intensity at the valley between two neighboring peaks in the SE curve was higher than that in the p-SE curve, indicating that the lateral resolution was poorer along the SE direction. Representative LSF curves for the SE (red dotted curve) and p-SE (black curve) directions are shown in Fig. 4(c). The lateral resolution was measured to be 1.64 ± 0.20 μm and 1.45 ± 0.10 μm for the SE and p-SE directions, respectively. The axial response curve is shown in Fig. 5. The axial resolution was measured to be 10 μm. The field curvature was measured to be 3 μm, which was smaller than the axial resolution. These

#192677 - $15.00 USD Received 21 Jun 2013; revised 1 Aug 2013; accepted 5 Aug 2013; published 13 Aug 2013

results showed that the 100-kHz SECM system provided similar optical resolutions to those obtained by the 5-kHz SECM system, which had a lateral resolution of 2 μm and an axial resolution of 10 μm. The sensitivity of the system was measured as 60 dB, which was high enough to image tissues with a reflectivity of −50 to −40 dB.

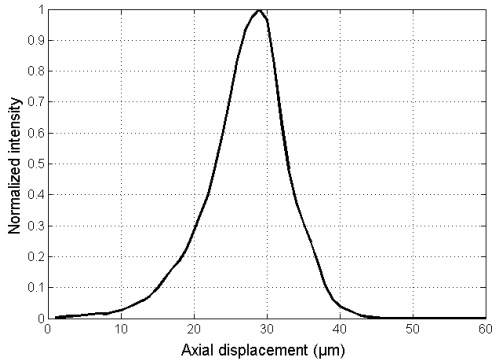

Fig. 5. Axial response curve.

3.3 Tissue imaging

SECM images of excised swine esophageal tissue taken at the imaging depths of approximately 150 μm are shown in Fig. 6. The large-area SECM image (Fig. 6(a)) visualizes papillae as dark openings (arrowheads). On higher magnification, the SECM image (Fig. 6(b)) clearly shows nuclei of squamous cells (arrows) surrounding a papillae located at the center of the image. SNR for the swine esophageal tissue image was measured to be 23.8 (14 dB).

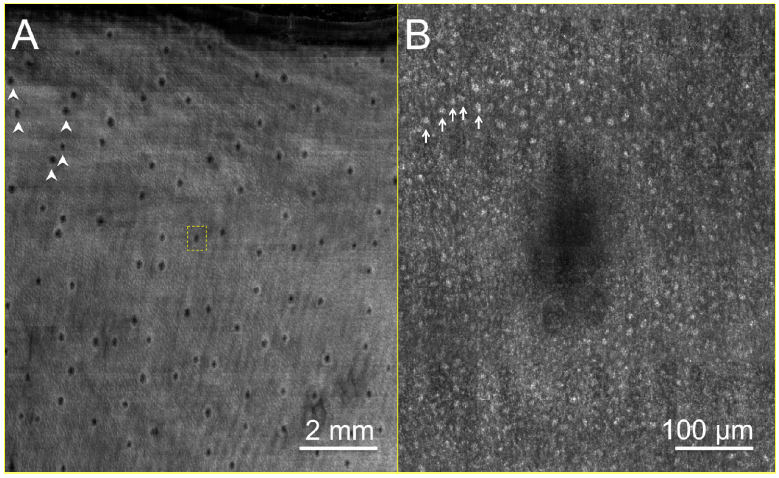

Fig. 6. SECM image of swine esophagus tissue: A. low-magnification SECM image obtained at the imaging depth of 150 μm; B. magnified view of the dotted box in (A). Arrowheads – papillae; Arrows – nuclei of squamous cells.

SECM images of a human esophageal tissue are shown in Fig. 7. In the low-magnification image (Fig. 7(a)), the architectural difference between the upper and lower parts of the tissue is noticed: the upper part exhibits glandular and foveolar architecture, while the lower part does not show any specific tissue architecture. The high-magnification image of the dotted box in the upper part of the tissue (Fig. 7(b)) shows the clear delineation between the lamina propria (LP) and epithelia (E). At an even higher magnification, the SECM image (Fig. 7(c)) allows the visualization of nuclei (arrows) of individual columnar cells. The high-magnification image of the dotted box in the lower part of the tissue (Fig. 7(d)) reveals that

#192677 - $15.00 USD Received 21 Jun 2013; revised 1 Aug 2013; accepted 5 Aug 2013; published 13 Aug 2013

this part of the tissue appears to have highly atypical architecture, with isolated cellular structures in the parenchyma, suggestive of intra-mucosal carcinoma (IMC). SNR for the EMR tissue image was measured as 29.4 (15 dB).

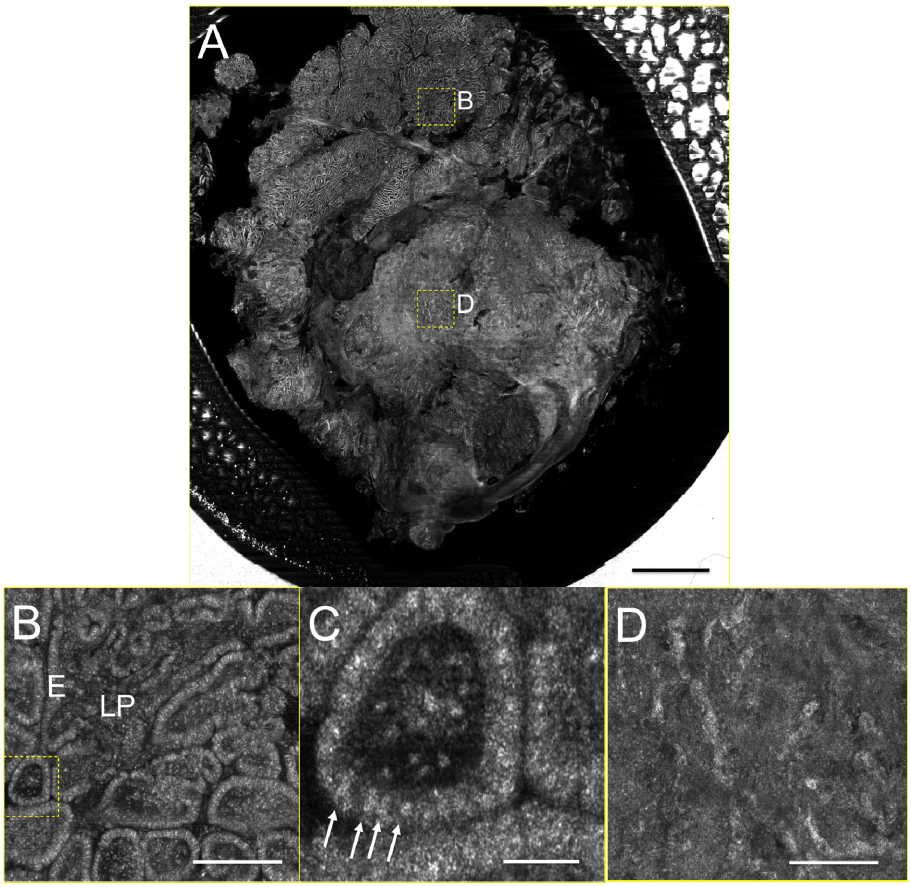

Fig. 7. SECM image of human esophagus tissue. A. low-magnification image; B. magnified view of the dotted box B in (A); C. magnified of the dotted box in (B); D. magnified view of the dotted box D in (A). E – epithelium; LP – lamina propria; Arrows – nuclei of columnar cells. Scale bars: A – 2mm; B and D – 300 μm, and C – 50 μm.

4. Discussion

The results described in this paper showed that large-area SECM imaging of esophageal tissues can be successfully conducted at the line imaging rate of 100 kHz. The 100-kHz SECM system had high sensitivity of 60 dB, which made it possible to image sub-surface cellular features of esophageal tissues with good SNR. The key cellular features visualized by SECM include papillae and nuclei of squamous cells in the normal swine tissue and villous architecture, nuclei of columnar epithelia cells, and intra-mucosal carcinoma in the diseased human tissue.

This imaging rate of 100 kHz can uniquely enable the imaging of a very large area of the esophagus *in vivo*. For the example described in the Introduction section, where the entire distal esophagus is imaged by an SECM endoscopic probe, the 100-kHz SECM system can reduce the imaging time from 12 minutes down to 37 seconds – and for a typical 5 imaging planes, the time will be reduced from one hour to three minutes. The short imaging time will make the SECM technology more practical for *in vivo* imaging of entire luminal organs in human subjects.

#192677 - $15.00 USD Received 21 Jun 2013; revised 1 Aug 2013; accepted 5 Aug 2013; published 13 Aug 2013

The actual imaging time demonstrated in this paper, however, was longer than the imaging time that the 100-kHz SECM system can achieve. With the scanning speed of 70 mm/sec for the fast translation stage and the scanning step size of 150 μm for the other translation stage, the theoretical imaging time for the imaging area of 10×10 mm^2 should be less than 10 sec. The acceleration and deceleration of the translation stage, however, increased the imaging time to 15 sec. During *in vivo* endoscopic imaging, we will rotate the SECM probe at a constant speed and will therefore be able to fully utilize the imaging speed of the 100-kHz SECM system.

The imaging rate can be increased further by using a faster swept source. A sweeping rate of 400 kHz is achievable by modifying the tunable filter and delay lines of the current source [17]. Multi-MHz sweeping rates can be achieved using Fourier domain mode locked (FDML) swept sources [18]. As described in the Methods section, we need to sample 256 pixels per spectrally-encoded line to achieve Nyquist sampling. The current detector unit has a bandwidth of 100 MHz, which is large enough to conduct Nyquist sampling of 256 pixels per line up to a line imaging rate of 390 kHz. The bandwidth of the detector unit can be increased to 150 MHz with an improved design of the post amplifier, which can allow a line imaging rate of 590 kHz. Future development of faster InGaAs detectors and electronics might allow even higher imaging rates.

As shown in the number 9 figure in the inset of Fig. 4(a), jitter occasionally appeared along the p-SE direction. In the DAQ unit, the signal was sampled by the internal clock, while the sampling was triggered by the external trigger pulse. The external trigger pulse was not synchronized with the internal clock, and this lack of synchronization caused the jitter shown in Fig. 4(a). The level of jitter was very low, 1 pixel, which corresponded to 0.27 μm. Since the nuclear size was 5 to 10 μm for both the swine and human esophageal tissues, the tissue images did not exhibit any noticeable artifacts caused by the jitter. Therefore, we expect that this low level of jitter will not adversely affect the image quality during the *in vivo* imaging of the esophagus. There, however, might be a need to reduce the jitter level further, for instance to visualize sub-nuclear features. We can increase the internal clock speed, which will reduce the pixel size. The jitter level will still be 1 pixel, but the jitter amount in the spatial coordinate will be reduced. This approach, however, will increase the number of samples per line and will subsequently increase the data size.

In conclusion, we have demonstrated large-area SECM imaging of esophageal tissues at a line imaging rate of 100 kHz. The SECM images enabled the visualization of sub-surface cellular structures of swine and human esophageal tissue *ex vivo*. In the next step of this research, we will develop a clinically-viable SECM endoscopic probe and use it with the 100-kHz SECM system for human esophageal imaging *in vivo*. The high imaging rate of 100 kHz will enable SECM imaging of the entire distal esophagus (5.0 cm) within a few minutes, providing a new paradigm for examining disease over the entire organ.

Acknowledgments

This research was supported by a sponsored research agreement with Nine Point Medical, Cambridge, MA. Dr. Schlachter is currently with Nine Point Medical. Dr. Woods is currently with Emory University Hospital, Atlanta, GA. Drs. Tearney and Bouma receive sponsored research from and consult for Nine Point Medical. Nine Point Medical has a licensing arrangement with Massachusetts General Hospital. Drs. Schlachter, Kang, Gora, Carruth, Bouma and Tearney have the right to receive royalties from this licensing arrangement.

#192677 - $15.00 USD Received 21 Jun 2013; revised 1 Aug 2013; accepted 5 Aug 2013; published 13 Aug 2013